

Determination of ultrathin diamond films by Raman spectroscopy

Leonid A. Chernozatonskii^{*1}, Boris N. Mavrin², and Pavel B. Sorokin^{1,3}

¹Emanuel Institute of Biochemical Physics, Russian Academy of Sciences, 4 Kosigina St., Moscow 119334, Russian Federation

²Institute of Spectroscopy of RAS, 5 Fizicheskaya St., Troitsk 142190, Moscow Region, Russian Federation

³Technological Institute of Superhard and Novel Carbon Materials, 7a Centralnaya Street, Troitsk 142190, Moscow Region, Russian Federation

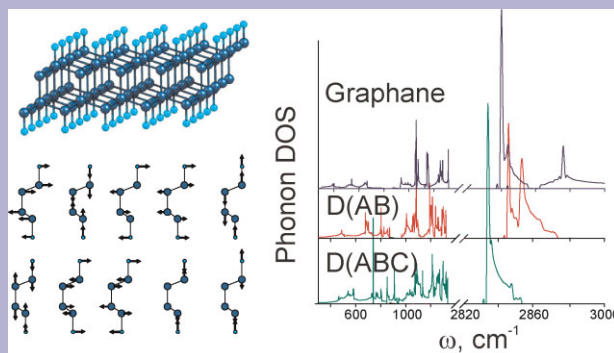
Received 29 September 2011, revised 6 February 2012, accepted 14 March 2012

Published online 11 April 2012

Keywords density functional theory, graphane, graphene, simulation of Raman spectroscopy, thin diamond films

* Corresponding author: e-mail cherno@sky.chph.ras.ru, Phone: +7-495-9397172, Fax: +7-499-1374101

The study of Raman spectra of recently predicted ultrathin diamond films (diamanes) with nanometer thickness, transformed from multilayered graphenes by the adsorption of hydrogen is presented. Here we studied the phonon spectra of diamane structures in detail by *ab initio* method, especially the Raman and infrared (IR) vibrational modes. In particular, two-layered diamanes display Raman peaks near 1110, 1260, 1320, 2860 cm^{-1} , and three-layered diamanes have a broad region (1110–1340 cm^{-1}) of Raman shifts and peaks near 2830–2860 cm^{-1} . The spectra are radically distinguished from the similar spectra of one to three layered graphenes and graphane.



Left side: Atomic structure and vibration pattern of optical modes of ultrathin diamond (diamane). Right: Phonon densities of the states of graphane and diamanes.

© 2012 WILEY-VCH Verlag GmbH & Co. KGaA, Weinheim

1 Introduction Raman spectroscopy has been historically used to probe the structural and electronic characteristics of carbon materials, as well as nanotubes and graphene [1, 2]. The major Raman features of graphene and graphite are the G band ($\sim 1580 \text{ cm}^{-1}$) bounded with in-plane sp^2 carbon atom vibrations, and 2D band ($\sim 2670 \text{ cm}^{-1}$) originated from a second-order process of phonons near the K-point. The D band ($\sim 1340 \text{ cm}^{-1}$) of defected graphene and graphite is close to the main diamond peak (1333 cm^{-1}).

Raman studies have been used also as a quick method for the determination of hydrogenization steps of one to five layered graphene [3]. Interest in this process appears in connection with the recent proposal [4, 5] and observation [6] of a graphane CH structure, hydrogenated graphene

with sp^3 -hybridized carbon atoms. After hydrogen plasma treatment the Raman spectrum of graphene changed significantly and three peaks at 1350, 1620, and 2950 cm^{-1} were observed [6].

The structures of other hydrocarbon films, so-called diamanes (C_2H or C_3H) have been predicted quite recently [7]. This result was proved in Refs. [8–10] where the stability and electronic properties of the C_2H films were also analyzed. In particular, in the paper [8] it was shown that C_2H structure can be synthesized by subsequent hydrogenation of bilayer graphene and in the paper [9] the fabrication of diamond films by binding of layers of hydrogenated multilayered graphene was analyzed. It should be noted that despite only a theoretical proposal of the existence of

hydrogenated ultrathin diamond films, the synthesis of bulk structure consisting of layers of fluorinated diamane was reported in the former experimental work [11], and in the recent paper [12] the electronic structure and stability of single fluorinated diamane film were analyzed.

The structures display interesting electronic and mechanical properties, e.g., the direct bandgap against the bulk diamond [7], therefore diamanes can be used as an active laser medium within lasers. Thus, the identification of such structures is currently important, especially because of observations of the unknown features of few-layered hydrogenated graphene, where two- and three-layered graphenes have been hydrogenized more perfectly (e.g., the intensity ratio of sp^3 - and sp^2 -hybridized carbon components of three-layered graphene is 0.5) [3].

In this paper, we present the results of the computational study of the phonon spectra of C_2H and C_3H ultrathin diamond films (see schemes in Fig. 1) and discuss their Raman spectra features and compare them with the available experimental data.

2 Methods and model For the calculation of the phonon spectra we used the first-principles approach based on DFT within the local density approximation for the exchange-correlation interaction as implemented in the PWSCF package [13]. Kohn–Sham orbitals are expanded in the plane waves with the use of ultrasoft pseudopotentials

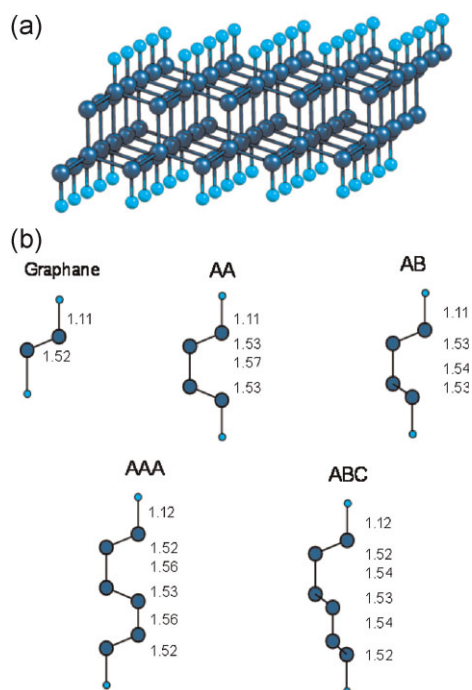


Figure 1 (online color at: www.pss-b.com) (a) The diamane D(AB) structure, the carbon atoms are marked in dark blue, the hydrogen atoms are marked in light blue. (b) The geometrical parameters of graphane, D(AA), D(AB), D(AAA), and D(ABC), the distance between the atoms is measured in angstroms

to describe the valence electrons, with 40 Ry cutoff energy for the wave functions and 480 Ry for the charge density. The calculations of vibration of the relaxed structures are performed in the linear response approximation with a Monkhorst–Pack grid of $6 \times 6 \times 1$ points. After the relaxation of the samples the forces acting on the atoms are lower than 10^{-2} eV/Å.

3 Results and discussion The calculations of the structures were made for isolated two- and three-layered diamond films. The cell lattice perpendicular to the diamane surface (c -axis) was chosen as 8 and 11 Å for two- and three-layered diamond films, respectively. Note that thickness is not a unique parameter for the description of the film structure because the films with the same thickness are distinguished by relative arrangement of consisted carbon layers. Ultrathin diamond films can be considered as the covalently bound stack of graphene sheets the stacking order of which governs the relative arrangement of the carbon layers in the films. For example, diamond film consisting of covalently bounded two-layered graphene with AB (Bernal) stacking differs from the film the structure of which originates from bilayer graphene with AA stacking. We classify the first and second film as D(AB) and D(AA), respectively. In general classification two-layered diamond film is named as $D(ij)$ (where ij can be equal to AB and AA), a three-layered film as $D(ijk)$ (where ijk can be equal to ABC, AAC, and AAA) and so on. Note that two- and three-layered graphene with AA and ABC stacking that can be used as base for the D(AA) and D(ABC) has been observed quite recently in Ref. [3] and Refs. [14, 15], respectively.

As an example, in Fig. 1a the structure of a two-layered diamane D(AB) is presented. Here, the carbon atoms of the sublattice A of the upper layer are bound with the hydrogen atoms and the atoms from the sublattice B of the upper layer are bound with the carbon atoms of the sublattice A of the lower layer, the atoms from the sublattice B of the lower layer are again bound with the hydrogen atoms, therefore all the carbon atoms in the diamane display sp^3 -hybridized state. The computed values of the bond lengths between the atoms are shown in Fig. 1b. The bond lengths of graphane (CH) are practically the same as in the reference work of Sofo et al. [5]. In Table 1 the geometrical data of the films are presented.

It should be mentioned that it is more difficult to synthesize large areas of graphene than of diamane. The hydrogen atoms adsorb on the surface of a single or multilayered graphene sheet randomly because of the equivalence of the atoms on different sublattices, therefore on the graphene two (or three [16]) different hydrogenated regions with the graphene boundaries between them can be formed. On the contrary, in the case of diamanes it can be favorable for the hydrogen atoms to bind to the chemically active carbon atoms situated on the surface layers of the multilayered graphene because such atoms do not have nearest neighbors under (over) surface layers. Because of this, only one graphene sublattice of each sheet can be

Table 1 Geometrical data of the structures investigated in this work.

name and notation	graphane	two-layered diamane, lonsdaleite structure D(AA)	two-layered diamane, diamond structure D(AB)	three-layered diamane, lonsdaleite structure D(AAA)	three-layered diamane, diamond structure D(ABC)
chemical formula	CH	C ₂ H	C ₂ H	C ₃ H	C ₃ H
symmetry	D _{3d} ³	D _{3h} ¹	D _{3d} ³	D _{3h} ³	D _{3d} ³
lattice constant, Å	2.518	2.509	2.512	2.4997	2.500
structural data	C 1/3 1/3 0.462 C-1/3 2/3 0.538 H 1/3 1/3 0.277 H-1/3 2/3 0.723	C-1/3 2/3 0.341 C 0 0 0.402 C 0 0 0.598 C-1/3 2/3 0.659 H-1/3 2/3 0.202 H-1/3 2/3 0.798	C-1/3 2/3 0.344 C 0 0 0.404 C 0 0 0.596 C 1/3 1/3 0.657 H-1/3 2/3 0.204 H 1/3 1/3 0.796	C 0 0 0.290 C-1/3 2/3 0.334 C-1/3 2/3 0.477 C 0 0 0.523 C 0 0 0.666 C-1/3 2/3 0.710 H 0 0 0.189 H-1/3 2/3 0.811	C 0 0 0.293 C-1/3 2/3 0.337 C-1/3 2/3 0.477 C 1/3 1/3 0.523 C 1/3 1/3 0.663 C 0 0 0.707 H 0 0 0.192 H 0 0 0.808

Note that the z coordinates are given for $c = 6, 8,$ and 11 Å in the cases of graphane, D(ij), and D(ijk), respectively.

covalently bound with hydrogen and therefore, the diamane regions of only one type can be formed.

The phonon spectra of all the structures presented in Fig. 1b were calculated but due to similarity of the phonon spectra of diamanes with different stacking order only the frequency dispersions of D(AB) and D(ABC) are shown in Fig. 2a and b.

A distinguishable feature of the phonon spectra of such structures is the presence of new phonon branches in the region around 1000 cm^{-1} absent in the case of graphane [5]. The phonon densities of states (PDOS) of diamanes also differ from the graphane PDOS (Fig. 2c): in the region of 1100 cm^{-1} new peaks are present and the high frequency

region (near 2800 cm^{-1}) is changed. The PDOS of D(AB) has two peaks at 2846 and 2854 cm^{-1} , while the PDOS of D(ABC) gives only one peak at 2834 cm^{-1} . This feature can help to distinguish D(ijk) from D(ij). Only D(AB) and D(ABC) PDOSs are shown in Fig. 2c due to the similarity of the densities of states of diamanes with the same thickness. We did not obtain the number of bands (G, D', 2D, and D + D' bands around $1580, 1620, 2680,$ and 2950 cm^{-1} frequencies, respectively) observed in graphane [6] because the G peak corresponds to the vibration of sp^2 carbon (graphene regions in experimentally synthesized graphane), D' corresponds to vibrations of defects of the lattice, and the 2D peak arises from a second-order process of phonons that

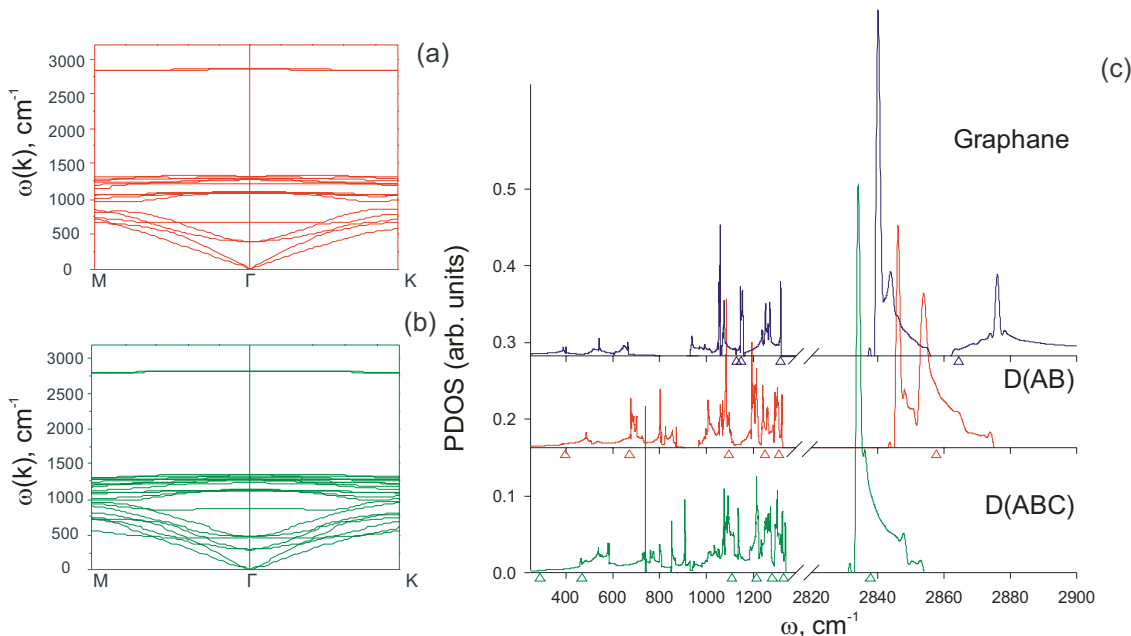


Figure 2 (online color at: www.pss-b.com) Phonon spectra of diamanes (a) D(AB) and (b) D(ABC). Only in-plane acoustic modes are shown. (c) Phonon density of states of graphane, diamane D(AB), and D(ABC). The higher-frequency modes correspond to C–H vibrations. Raman-active modes are highlighted by triangles.

cannot be obtained in our simulations. The bands calculated in the regions of 2800 cm^{-1} correspond to vibration of hydrogen atoms in the in-plane direction, not observed in experiment because such vibration can be also obtained by in-plane excitation of graphane.

In the paper [17] the study of Raman spectra of diamond nanoclusters was carried out. The authors found that the strongest Raman peaks occurred in the vicinity of 1200, 1500, and $350\text{--}550\text{ cm}^{-1}$ which coincides with our results (see Fig. 2c). Additional support to our data is provided in Ref. [18] where the Raman spectrum of graphane was computed. The obtained frequencies of active Raman modes perfectly correspond with our calculations.

The vibration patterns of optical modes for graphane and $D(ij)$ and $D(ijk)$ structures are represented in Fig. 3. Among these modes, the eigenvectors of the nondegenerate modes are perpendicular to layers, while the eigenvectors of the degenerate modes are parallel to layers. The zero-wave values of the phonon frequencies in the Brillouin zone center of diamane $D(AA)$, $D(AB)$, $D(AAA)$, $D(ABC)$ films are presented in Table 2. The $D(ijk)$ peak of the E_g (R) mode is higher than that of the $D(ij)$ peak by at least 14 cm^{-1} , indicating the stiffening of the lattice that can be used in the

Table 2 Frequencies (in cm^{-1}) of Raman (R) and infrared (IR) modes for diamanes $D(ij)$ and $D(ijk)$.

AA, D_{3h}	AB, D_{3d}	AAA, D_{3d}	ABC, D_{3d}	assignment
372, E'' (R)	398, E_g (R)	273	292	E_g (R)
		459	484	E_u (IR)
691, $A_1'A_1'$ (R)	676, A_{1g} (R)	482	472	A_{1g} (R)
1098, E'' (R)	1103, E_g (R)	868	858	A_{2u} (IR)
		1118	1119	E_g (R)
1106, E' (R, IR)	1108, E_u (IR)	1118	1123	E_u (IR)
1205, A_2'' (IR)	1210, A_{2u} (IR)	1212	1224	A_{1g} (R)
1227, A_1' (R)	1259, A_{1g} (R)	1235	1258	A_{2u} (IR)
1267, E'' (R, IR)	1275, E_u (IR)	1246	1262	E_u (IR)
1319, E'' (R)	1320, E_g (R)	1260	1293	A_{1g} (R)
		1311	1316	E_u (IR)
		1334	1342	E_g (R)
2866, A_1' (R)	2857, A_{1g} (R)	2849	2830	A_{2u} (IR)
2875, A_2'' (IR)	2864, A_{2u} (IR)	2854	2837	A_{1g} (R)

Here the bold letters are determined by modes correlated with three-degenerated F_{2g} diamond mode: the last transforms into two modes ($F_{2g} \rightarrow A_{1g} + E_{2g}$).

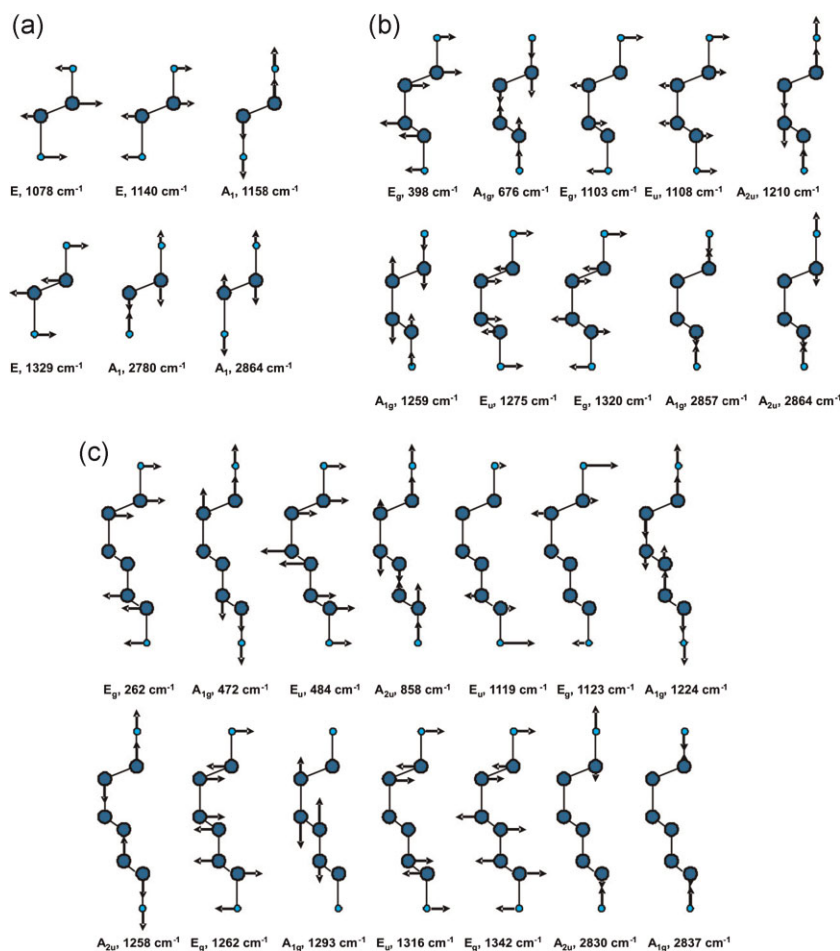


Figure 3 (online color at: www.pss-b.com) Eigenvectors of (a) graphane, (b) diamane $D(AB)$, and (c) $D(ABC)$ at the Γ -point.

determination of the number of layers in the diamonds similar to using the second-order Raman band to confirm the presence of one-, two-, and three-layered graphenes [1]. For diamond D(AA), the D_{3h} point group is not a subgroup of the group O_h of diamond and between their presentations any correlation is absent; the 1106 and 1267 cm^{-1} frequencies are permitted by the symmetry for the Raman and infrared (IR) modes. The peaks near 2830–2860 cm^{-1} mainly coincide with the vibrations of the hydrogen atoms. The comparison of the Raman spectra of two- and three-layered graphenes [1] and the spectra of the studied diamonds allows one to clearly identify the presence of the diamond structures in the experiment.

The results presented here are highly relevant to the application of transformed two- and three-layered graphene in nanoelectronics (as the thinnest dielectrics the properties of which can be tuned by doping by different elements, for example, N or B) and nanomechanic devices (as very strong films with nanometer thickness) and aids in better understanding of the physical and electronic properties of thin diamond-like films. A possible preparation of diamond can be similar to graphane synthesis schemes using a high-pressure hydrogen flow in the H-plasma method [3, 6].

Acknowledgements Our work was performed using ‘Lomonosov’ supercomputer of Moscow State University and Joint Supercomputer Centre of the Russian Academy of Sciences. The work was supported by the Russian Foundation for Basic Research (project no. 11-02-01453a), and Russian Ministry of Education and Science (Contract No. 16.552.11.7014).

References

- [1] A. C. Ferrari, J. C. Meyer, V. Scardaci, C. Casiraghi, M. Lazzeri, F. Mauri, S. Piscanec, D. Jiang, K. S. Novoselov, S. Roth, and A. K. Geim, *Phys. Rev. Lett.* **97**, 187401 (2006).
- [2] D. Graf, F. Molitor, K. Ensslin, C. Stampfer, A. Jungen, C. Hierold, and L. Wirtz, *Nano Lett.* **7**, 238 (2007).
- [3] Z. Luo, T. Yu, K. Kim, Z. Ni, Y. You, S. Lim, Z. Shen, S. Wang, and J. Lin, *ACS Nano* **3**, 1781 (2009).
- [4] M. H. F. Sluiter and Y. Kawazoe, *Phys. Rev. B* **68**, 085410 (2003).
- [5] J. O. Sofo, A. S. Chaudhari, and G. D. Barber, *Phys. Rev. B* **75**, 153401 (2007).
- [6] D. C. Elias, R. R. Nair, T. M. G. Mohiuddin, S. V. Morozov, P. Blake, M. P. Halsall, A. C. Ferrari, D. W. Boukhvalov, M. I. Katsnelson, A. K. Geim, and K. S. Novoselov, *Science* **323**, 610 (2009).
- [7] L. A. Chernozatonskii, P. B. Sorokin, A. G. Kvashnin, and D. G. Kvashnin, *JETP Lett.* **90**, 134 (2009).
- [8] O. Leenaerts, B. Partoens, and F. M. Peeters, *Phys. Rev. B* **80**, 245422 (2009).
- [9] L. Zhu, H. Hu, Q. Chen, S. Wang, J. Wang, and F. Ding, *Nanotechnology* **22**, 185202 (2011).
- [10] D. K. Samarakoon and X. Q. Wang, *ACS Nano* **4**, 4126 (2010).
- [11] H. Touhara, K. Kadono, Y. Fujii, and N. Watanabe, *Z. Anorg. Allgem. Chem.* **544**, 7 (1987).
- [12] M. A. Ribas, A. K. Singh, P. B. Sorokin, and B. I. Yakobson, *Nano Res.* **4**, 143 (2011).
- [13] P. Giannozzi, S. Baroni, N. Bonini, M. Calandra, R. Car, C. Cavazzoni, D. Ceresoli, G. L. Chiarotti, M. Cococcioni, I. Dabo, A. D. Corso, S. de Gironcoli, S. Fabris, G. Fratesi, R. Gebauer, U. Gerstmann, C. Gougousis, A. Kokalj, M. Lazzeri, L. Martin-Samos, N. Marzari, F. Mauri, R. Mazzarello, S. Paolini, A. Pasquarello, L. Paulatto, C. Sbraccia, S. Scandolo, G. Sclauzero, A. P. Seitsonen, A. Smogunov, P. Umari, and R. M. Wentzcovitch, *J. Phys.: Condens. Matter* **21**, 395502 (2009).
- [14] C. H. Lui, Z. Li, Z. Chen, P. V. Klimov, L. E. Brus, and T. F. Heinz, *Nano Lett.* **11**, 164 (2011).
- [15] C. Cong, T. Yu, K. Sato, J. Shang, R. Saito, G. F. Dresselhaus, and M. S. Dresselhaus, *ACS Nano* **5**, 8760 (2011).
- [16] V. I. Artyukhov and L. A. Chernozatonskii, *J. Phys. Chem. A* **114**, 5389 (2010).
- [17] D. Zhang and R. Q. Zhang, *J. Phys. Chem. B* **109**, 9006 (2005).
- [18] H. Şahin, M. Topsakal, and S. Ciraci, *Phys. Rev. B* **83**, 115432 (2011).